JOURNAL OF MATERIALS SCIENCE 23 (1988) 4445–4449

# Surface layers produced by ion nitriding of austenitic Fe–Mn–Al alloys and the effects on hardness and corrosion resistance

K. SATO, K. TAKAHASHI, Y. INOUE
*Analysis Center, The Technological University of Nagaoka, Nagaoka, Niigata 940-21, Japan*
T. YAMAZAKI
*Department of Industrial Chemistry, Tsuruoka Technical College, Tsuruoka, Yamagata 997, Japan*
Y. NITOH
*Yamagata Research Institute of Technology, Yamagata 990, Japan*

Austenitic (fcc) Fe–Mn–Al alloys were nitrided in the temperature range 723 to 973 K by a glow discharge method using $H_2$–$N_2$ gas mixtures, and the microstructures and compositions of the nitrided layers were investigated in detail. A thin surface layer and a thick nitrogen-diffused layer (internal nitrided layer) were produced; the former consisted of both manganese nitrides and a ferritic (bcc) phase, while the internal nitrided layer had an austenitic structure with the incorporated excess nitrogen atoms. X-ray photoelectron spectra revealed that the incorporated nitrogen atoms have a strong interaction with aluminium lattice atoms. By nitriding, hardness values of the Fe–Mn–Al alloys were increased from $H_V$ = 350 to ca. 1000, and the corrosion resistance to sulphuric acid solution was enhanced by a factor of 30. These improvements are associated with a uniform distribution of the incorporated nitrogen and also with the presence of nitride-like interactions between the nitrogen and aluminium atoms.

## 1. Introduction

Fe–Mn–Al alloys are considered to be possible substitutes for the Ni–Cr austenitic stainless steels [1–4]. The replacement of nickel by manganese in ferrous alloys can afford a stable austenitic structure, and the moderate addition of aluminium to higher-manganese steels can lead to the stability of the austenitic phase against the $\gamma \rightarrow \varepsilon$ martensitic transformation [2, 5]. Although the Mn–Al steels possess excellent mechanical properties, it seems that the corrosion and oxidation properties of these steels are somewhat inferior to those of the conventional austenitic Ni–Cr stainless steels [4]. Thus, the improvement of these properties has become an important subject.

One of the effective ways is a surface modification, nitriding, a technique which has been widely adopted to improve fatigue and abrasive resistance and also to increase the anti-corrosion properties of steels. The nitriding of steels is promoted by the presence of alloying elements with a stronger nitrogen affinity such as aluminium, chromium and titanium. In austenitic Fe–Mn alloys the solubility of nitrogen increases with increasing amount of manganese [6]. Thus, austenitic Mn–Al steels are alloys suitable for nitriding in order to improve their abrasive and corrosion resistance, but little work on the structures of the nitrided layer compounds as well as on their chemical and mechanical properties has been done so far.

In the present study, a d.c. glow discharge method was used for nitriding the alloys. Nitriding conditions such as temperature and the gaseous composition of the active plasma were varied extensively, and the structures of the layer compounds produced were characterized by means of X-ray diffraction, X-ray photoelectron spectroscopy (XPS), scanning electron microscopy (SEM) and X-ray microanalysis (XMA). In addition, the mechanism of formation of the layer compounds was investigated. In relation to the properties of the nitrided alloys, the corrosion resistance and hardness were briefly examined.

## 2. Experimental procedure

Four kinds of austenitic Fe–31.3 wt % Mn, Fe–19.1 wt % Mn–1.8 wt % Al, Fe–29.1 wt % Mn–2.1 wt % Al, and Fe–29.2 wt % Mn–3.8 wt % Al alloys were used as specimens. Before nitriding these alloys were electropolished (10 V, 8 to 10 mA) in chromic–phosphoric acid solution and then ultrasonically cleaned in acetone. Nitriding treatment was performed by means of a d.c. glow discharge method in which the alloy samples were placed in the cathode position. Prior to ion nitriding, the samples were subjected to etching by hydrogen sputtering for 10 min, unless otherwise specified, to remove surface contaminants. After this sputter cleaning, a mixture of nitrogen and hydrogen gas to generate an active plasma was introduced, and a d.c. voltage was applied between the samples and the anode (the wall of the reaction

0022–2461/88 $03.00 + .12 

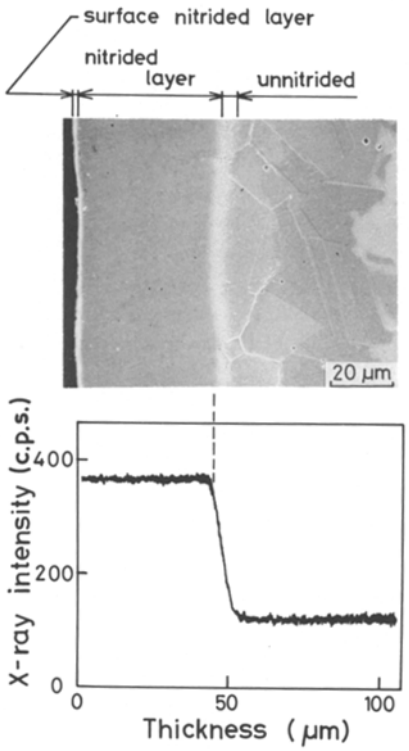


*Figure 1* Scanning electron micrograph of a cross-section and X-ray elemental line profile of nitrogen (N$K\alpha$) for nitrided Fe–29 wt % Mn–3.8 wt % Al. Nitriding conditions: $T = 773$ K, $t = 20$ h, $H_2/N_2 = 9$.

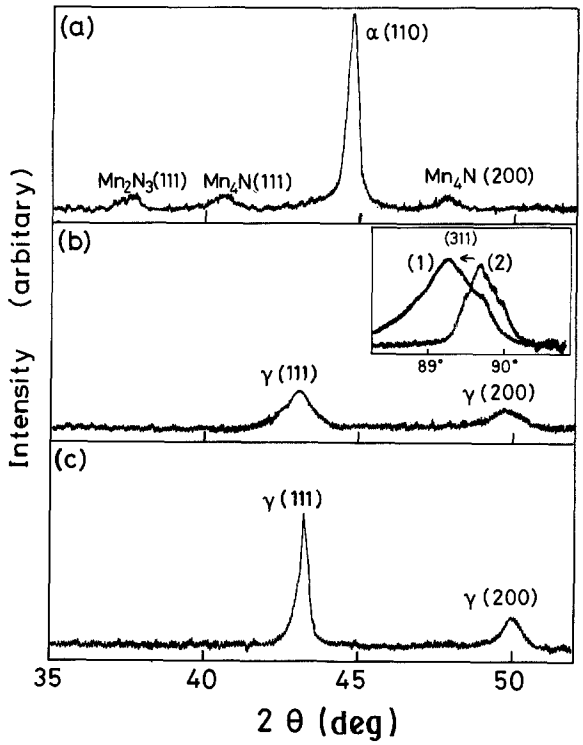


*Figure 2* X-ray diffraction patterns of the phases produced by ion-nitriding. The sample was prepared in the same conditions as shown in Fig. 1. (a) Surface nitrided layer. (b) Internal nitrided layer; the inset shows the peak shift and line broadening of the $\gamma$ (3 1 1) peak (1) in comparison with that of the unnitrided alloy (2). (c) Unnitrided austenite phase.

chamber). The nitriding gases were a preset mixture of high purity $H_2$ (99.999%) and $N_2$ (99.99%): the ratio of $H_2$ to $N_2$, $H_2/N_2$, was varied from 0.33 to 9 in volume percentage under 5 Torr of constant total pressure. The applied d.c. voltages and currents were respectively 250 to 490 V and 0.3 to 1.2 A. The nitriding temperatures of the samples were 723 to 973 K and were measured with a pyrometer.

The microstructures and layer compounds of the nitrided alloys were analysed by an X-ray diffractometer (Rigaku RAD-IIIA), an X-ray microanalyser with SEM (Jeol JXA-733), and an X-ray photoelectron spectrometer (Jeol JPS-100SX). The microhardness of the nitrided alloys was measured as a function of depth from the surface to the interior by use of a Vickers hardness indenter. The corrosion tests were carried out in 0.1 N sulphuric acid solution at room temperature by using an a.c. impedance corrosion monitor (Rigaku) to measure the corrosion rate of the specimen [7]. The frequencies of the sinusoidal waves, a.c. voltage and surface area of the electrode metal were 20 kHz, 0.017 Hz, 7 mV and 80 $mm^2$, respectively.

## 3. Results

### 3.1. Microstructures and layer compounds formed in the nitrided alloys

Fig. 1 shows the microstructure and concentration profile of nitrogen in the nitrided layers produced after nitriding of the Fe–29 wt % Mn–3.8 wt % Al alloy for 20 h at 773 K in a mixture of $H_2/N_2 = 9$. The general features of the microstructure are the formation of an outer thin surface layer (surface nitrided layer) and a thick unetched layer (internal nitrided layer), both of which grow parallel to the surface. These structures are similar regardless of the alloy composition. The depth profile of nitrogen by the XMA line analysis showed that in the internal nitrided layer the nitrogen level was high and almost constant, and a narrow diffusion zone was formed between the nitriding front and the unnitrided $\gamma$-austenite phase. The concentrations of iron, manganese and aluminium in the nitrided region were also constant but were slightly lower than those in the unnitrided region. These results indicate that a relatively large amount of nitrogen atoms can be incorporated in the $\gamma$-austenite matrix by the ion nitriding.

Fig. 2 shows X-ray diffraction patterns for the nitrided layers and the unnitrided austenite phase of the same specimen as shown in Fig. 1. It is found that the outer thin surface layer with a thickness of a few micrometres consisted of both an $\alpha$-ferrite (b c c) and manganese nitrides ($Mn_4N$ and $Mn_2N_3$). The formation of the manganese nitrides become prominent at temperatures higher than about 770 K. On the other hand, the X-ray diffraction patterns for the internal nitrided layers were similar to those of the $\gamma$-austenite (f c c) matrix reflections but the peaks became broader and their positions shifted slightly toward lower diffraction angles, compared with the $\gamma$-reflections of the unnitrided alloys (Fig. 2b).

When Fe–29 wt % Mn–2.1 wt % Al alloy was nitrided at a temperature as high as 973 K at $H_2/N_2 = 0.33$ without hydrogen pre-sputtering, the X-ray diffraction patterns showed that relatively strong peaks due to MnO were present in addition to the reflections of the $\alpha$-ferrite and $\gamma$-austenite phases. Fig. 3 shows a scanning electron micrograph of a cross-section of the

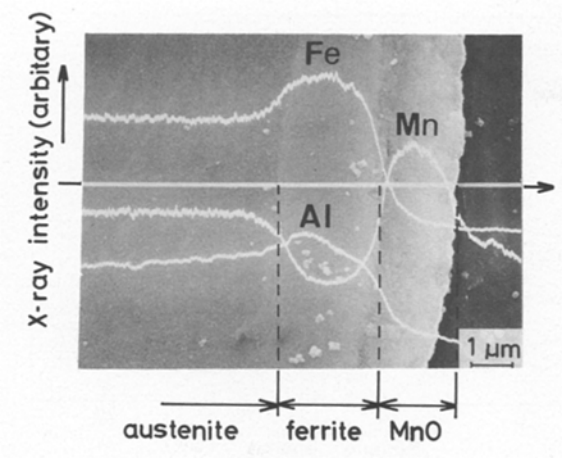


*Figure 3* Scanning electron micrograph of nitrided Fe–29 wt % Mn–2.1 wt % Al alloy and its X-ray elemental line profile analyses. Nitriding conditions: $T$ = 973 K, $t$ = 20 h, $H_2/N_2$ = 0.33 and without $H_2$ pre-sputtering.

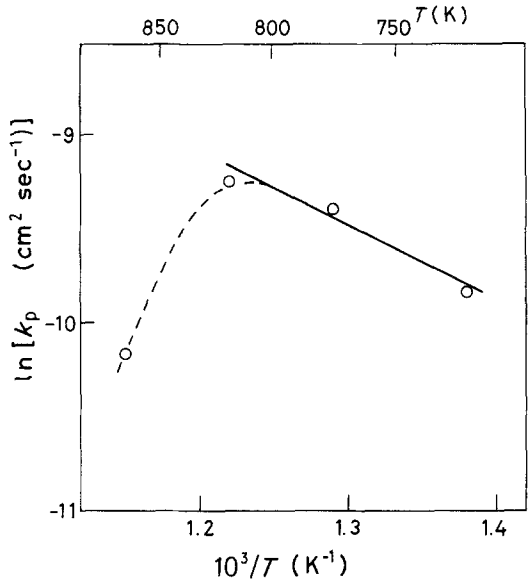


*Figure 4* Relationship between the reaction rate constant $k_p$ and reciprocal temperature for the nitriding reaction of Fe–29 wt % Mn–3.8 wt % Al alloy ($H_2/N_2$ = 9).

nitrided alloy, together with the X-ray elemental line profiles of the constituent alloy elements. From the surface to the interior, there existed a manganese-rich surface layer (MnO), a manganese-depleted layer which is the $\alpha$-ferrite phase, and an unreacted austenite phase. This indicates that the formation of MnO on the outermost surface layer impeded the nitriding reaction and resulted in a decrease of the nitrided layer. However, the formation of the surface MnO layer was drastically depressed either by the treatment of hydrogen pre-sputtering or by a lowering of the nitriding temperature. Furthermore, an increase in the $H_2/N_2$ ratio was also effective in eliminating the MnO layer, because the formation of manganese nitride compounds such as $Mn_2N_3$ and $Mn_4N$ was preferred to that of manganese oxides in the surface region. In the following experiments on the mechanical and chemical properties of the nitrided layers, the samples were prepared under the conditions under which no MnO layer was formed.

### 3.2. Nitriding layer formation

The formation of the nitrided layers as a function of time in the temperature range 723 to 873 K was examined for the Fe–29 wt % Mn–3.8 wt % Al alloy. The relationship between the layer thickness $x$ and the nitriding time $t$ obeyed a parabolic rate law $x^2 = k_p t$, where $k_p$ is the rate constant. These results imply that the nitriding rates are controlled by nitrogen diffusion through the austenite matrix. The plot of the logarithm of $k_p$ against $1/T$ shows a linear relationship below 820 K but deviated considerably at higher temperatures, as shown in Fig. 4.

### 3.3. XPS results on the nitrided layer

XPS measurements were conducted for the internal nitrided layer in order to reveal the interaction of the incorporated nitrogen atoms with the surrounding lattice atoms. For comparison, XPS spectra were also recorded for the unnitrided Fe–Mn–Al alloys. Prior to XPS analysis, the samples were mechanically polished to remove the surface thin layers and then were subjected to sputter-etching by argon ion bombardment at 500 eV in the XPS spectrometer to prepare clean surfaces.

Fig. 5 shows the XPS spectra of N 1s and Al 2p on the internal nitrided layers of the Fe–19 wt % Mn–1.8 wt % Al alloy nitrided at 773 K for 20 h. The N 1s line appeared at 396.8 eV, which is near that of AlN [8], when the binding energies were referenced to the Al 2p level of clean metallic aluminium. The similarity of binding energy and the almost symmetrical shape of the N 1s peak strongly suggest that almost all of the incorporated nitrogen is in a form of nitride. The Al 2p peak appeared at 73.5 eV for the nitrided layer. This layer also showed that the O 1s peak was hardly detected. The binding energy of Al 2p was larger by 1.5 eV than that of the unnitrided Fe–Mn–Al alloy (72.0 eV) and was similar to that of AlN [8]. Thus, these results clearly indicate that aluminium atoms have a nitride-like interaction with the incorporated nitrogen atoms. Manganese atoms are another possible candidate for interacting with the nitrogen atoms. However, there is an indication that the manganese atoms remain in a metallic state in the nitrided layer, although this assignment is obscured by severe overlapping of Mn 2p peak with that of the Fe (*KLL*) Auger transition. The binding energies of the Fe 2p level for the internal nitrided layer were almost the same as those of metallic iron, thus suggesting either that only small fractions of the iron lattice atoms have interactions with the incorporated nitrogen atoms or that the interaction between them was considerably weak. The nitrogen concentrations in the nitrided layer were estimated from the XPS peak area for several nitrided Fe–19 wt % Mn–1.8 wt % Al alloys by using Scofield's cross-section values [9], and it was derived that the nitrided alloys contain 4 to 6 at % nitrogen atoms.

### 3.4. Microhardness profiles

Typical hardness profiles for Fe–31 wt % Mn and Fe–29 wt % Mn–3.8 wt % Al alloys nitrided at 823 K are presented in Fig. 6. The constant hardness in the

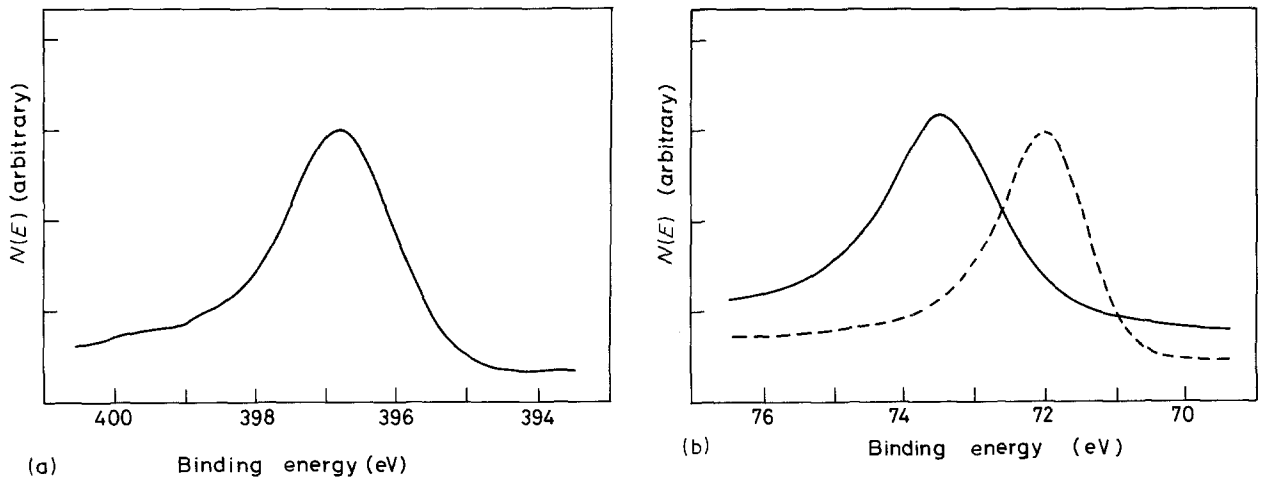


*Figure 5* XPS spectra of the internal nitrided layer. Solid lines: (a) N 1s and (b) Al 2p for Fe–19 wt % Mn–1.8 wt % Al alloy nitrided at 773 K for 20 h in $H_2/N_2 = 9$. Broken line: Unnitrided Fe–Mn–Al alloy.

internal nitrided layer was followed by an abrupt decrease at a certain thickness depending on the kind of alloy, and it is clearly shown that both the thickness of the hard layer and its hardness were raised by a factor of approximately two for the nitrided alloys containing aluminium atoms ($H_V$ = 950 to 1050). It is to be noted that the thickness of the hard layer was consistent with that of the internal nitrided layer.

### 3.5. Corrosion tests

The corrosion behaviour was compared for the Fe–29.2 wt % Mn–3.8 wt % Al alloy before and after nitriding for 20 h at 823 K. Both samples were immersed in 0.1 N sulphuric acid solution for 10 min and then a.c. voltages were applied. Fig. 7 shows that the values of the Faradaic corrosion resistance, $R_c$, increased with time and attained almost steady levels. A comparison of these saturated values indicates that the corrosion resistance became ca. 30 times higher for the nitrided alloy than for the unnitrided one. The Faradaic corrosion resistance can be reduced to the corrosion rate, i.e. the corrosion current density $I_{corr}$ of the metal investigated. By ion nitriding, the values of $I_{corr}$ for the Fe–29 wt % Mn–3.8 wt % Al greatly decreased from 2.25 to 0.0651 mA cm$^{-2}$. These decreases were also observed for other austenitic Fe–Mn–Al alloys. It is to be noted that ion nitriding of the austenitic Fe–Mn–Al alloys significantly enhances their corrosion resistance in sulphuric acid solution. This is in contrast to the behaviour observed for Ni–Cr stainless steels in which the corrosion resistance was reduced remarkably [10].

## 4. Discussion

The present study on Fe–Mn–Al alloys treated by the glow discharge of an $N_2$–$H_2$ gas mixture shows that the nitrided layers are divided into (i) a thin surface layer composed of manganese nitrides ($Mn_2N_3$ and $Mn_4N$) and an α-ferrite phase, and (ii) a thick inner diffusion layer (an internal nitrided layer) of nitrogen. The latter layer is particularly important, since it is clearly envisaged that this layer is responsible for the remarkable improvements of hardness and corrosion

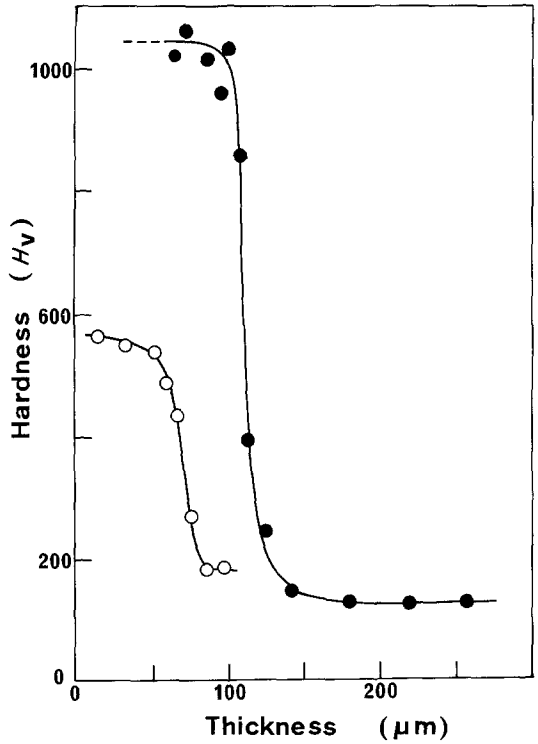


*Figure 6* Microhardness profiles for the internal nitrided layers of (○) Fe–31 wt % Mn and (●) Fe–29 wt % Mn–3.8 wt % Al alloys. Nitriding conditions: $T$ = 823 K, $t$ = 50 h, $H_2/N_2 = 9$.

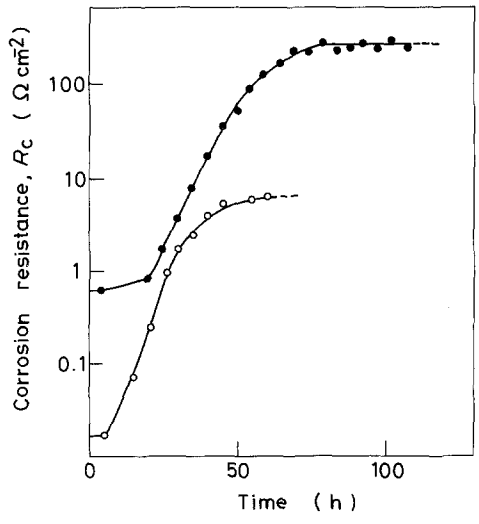


*Figure 7* Changes in a.c. impedance of (○) unnitrided and (●) nitrided Fe–29 wt % Mn–3.8 wt % Al alloys. Nitriding conditions: $T$ = 823 K, $t$ = 20 h, $H_2/N_2 = 9$.

resistance. As shown in Fig. 2b, broadening and shift of the X-ray diffraction peaks occurred in the $\gamma$ (f c c) lattice reflections for the internal nitrided layer. This is indicative of a lattice distortion due to the incorporation of nitrogen atoms beyond the limits of solid solution (e.g. ca. 0.5 wt % (2 at %) in an austenitic Fe–30 wt % Mn alloy at 823 K [16]).

The growth of the internal nitrided layer was strongly related to the properties of the surface layers. On nitriding at temperatures higher than 873 K, manganese oxide was produced on the outermost surface layer in addition to the formation of $\alpha$-ferrite phase. This oxide depressed the formation of the nitrided layer as is demonstrated in the lower $k_p$ value at 923 K in Fig. 4. Manganese metal atoms are very sensitive to oxygen; it is reported that manganese-rich oxide scales are readily produced in Fe–Mn alloys [11]. In the present Fe–(20 to 30) wt % Mn–Al alloys, a partial pressure of oxygen as low as $1.4 \times 10^{-12}$ Pa [12] is thermodynamically sufficient to produce stable MnO at 973 K, provided that the effects of reducing atmospheres are not taken into account. Thus, it seems difficult at the present time to remove oxygen to the extent of such a low limit, since traces of oxygen come from the introduced plasma gas as impurity, leaks from the surrounding atmosphere and/or contaminants such as $CO_2$, CO and $H_2O$ adsorbed on the chamber wall. However, the formation of MnO can be completely depressed when one chooses ion nitriding conditions such as a pre-sputtering by hydrogen prior to nitriding, a higher ratio of $H_2/N_2$ gas mixture and nitriding temperatures below about 820 K. These conditions correspond to attenuation of the residual oxygen sources and to an increase in reducing atmosphere. Thus, it is reasonable to consider that reducing species like $NH_x^+$ and $H^+$ ions in the active plasma play an important role in removing the influence of oxygen.

The kinetic behaviour showed that the formation of the internal nitrided layer obeyed a parabolic rate law. Furthermore, constant concentration profiles of nitrogen atoms in the nitrided layer were obtained (Fig. 1). Thus, it is considered that the rate-determining step of the layer growth is the diffusion of nitrogen through the $\gamma$-austenite matrix in accordance with internal nitriding theory [13]. The activation energy of the nitriding reaction can be obtained from the slope of the linear temperature dependence below 823 K in Fig. 4. For the Fe–29 wt % Mn–3.8 wt % Al alloy, the activation energy was 83 kJ mol$^{-1}$ which was considerably smaller than the values of 143 kJ mol$^{-1}$ [14] and 169 kJ mol$^{-1}$ [15] reported previously for nitrogen diffusion in austenitic iron. The low value is probably associated with differences in the interaction of nitrogen atoms with the surrounding matrix atoms. The XPS spectra showed that the nitrogen atoms have a somewhat nitride-like interaction with the aluminium atoms but not appreciably with iron and manganese and atoms. The XPS peak area for the internal nitrided layer suggested that the fraction of the incorporated nitrogen atoms is 4 to 6 at %, which is slightly larger than the bulk fraction of aluminium atoms (3.6 at %). Thus, it is likely that the nitrogen atoms are accommodated in the octahedral interstices of the f c c lattice sites where such chemical interactions between them become possible.

With respect to the corrosion resistance, a contrasting behaviour was observed between the present nitrided Fe–Mn–Al alloys and other common alloys. In the cases of stainless steels [16] and Fe–Ti alloys [17], it was observed that nitriding produced nitride precipitates such as CrN, $Cr_2N$ and $TiN_x$ in the inner diffusion layers. Since a kind of electrochemical local unit cell is made up between these nitride precipitates and the matrix elements, the presence of such precipitates promotes the extrusion of the metallic constituents under corrosion conditions, thus lowering the anti-corrosion properties. On the other hand, there was no clear indication of the formation of nitride particles in the nitrided Fe–Mn–Al alloys.

From the considerations mentioned above, it is concluded that the higher hardness and improvements of corrosion resistance are brought about by the uniform distribution of incorporated excess nitrogen and by its strong interaction with the aluminium atoms, which is considered to be analogous in nature to compounds such as $AlN_x$.

## Acknowledgements

The authors gratefully acknowledge the support and encouragement of Professor T. Kusakawa at Waseda University and Professor M. Ueno at the Technological University of Nagaoka. The experimental support and supply of alloys by Drs M. Yamanaka, M. Tendoh and I. Kimura of Nippon Steel Corporation, R&D Laboratory, are also acknowledged. This work is supported by a Grant-in-Aid for Developmental Scientific Research (No. 59 850 118) from the Ministry of Education, Science and Culture.

## References

1. S. BANERJI, *Met. Progr.* April (1978) 59.
2. J. CHARLES, A. BERGHEZAN, A. LUTTS and P. L. DANCOISNE, *ibid.* May (1981) 71.
3. J. GARCIA, N. ROSS and R. J. RIOJA, *ibid.* August (1982) 47.
4. R. WANG and F. H. BECK, *ibid.* March (1983) 72.
5. M. ICHNOSE, K. SATO, Y. INOUE, M. UENO and I. KIMURA, *Trans. Iron Steel Inst. Jpn* **25** (1985) B31.
6. V. RAGHAVAN, *Trans. Indian Inst. Met.* **37** (1984) A.
7. S. HARUYAMA, T. TSURU and M. ANAN, *Bo-shoku Gizyutsu* (in Japanese) **27** (1978) 449.
8. J. A. TAYLOR and J. W. RABALAIS, *J. Chem. Phys.* **75** (1981) 1735.
9. J. H. SCOFIELD, *J. Electron Spectrosc.* **8** (1976) 129.
10. K. ICHII, K. FUJIWARA and T. TAKASE, *Heat-treatment* (in Japanese) **25** (1985) 191.
11. J. P. SAUER, R. A. RAPP and J. P. HIRTH, *Oxid. Met.* **18** (1982) 285.
12. J. F. ELLIOT and M. GEISER, "Thermochemistry for Steelmaking", Vol. 1 (Addison-Wesley, 1960).
13. C. WAGNER, *Z. Elektrochem.* **63** (1959) 772.
14. P. GRIEVESON and E. T. TURKDOGAN, *Trans. AIME* **230** (1964) 407.
15. A. BRAMLEY, *Carnegie School Mem.* **15** (1926) 115.
16. B. BILLION and A. HENDRY, *Surf. Engng.* **1** (1985) 114.
17. D. S. RICKERBY, S. HENDERSON, A. HENDRY and K. H. JACK, *Acta Metall.* **34** (1986) 1687.

*Received 9 October 1987*
*and accepted 10 February 1988*